UMICore – A Mobile Radio Physical Layer Demonstrator

Benedikt Eschbach, Annika Böttcher and Peter Vary
Institute of Communication Systems and Data Processing (IND)
RWTH Aachen University, Germany
Email: {eschbach,boettcher}@ind.rwth-aachen.de

***Abstract*—This article presents UMICore, a software tool for the demonstration and visualization of various physical layer concepts as well as various channel models. The capabilities of UMICore are illustrated using UMTS LTE as exemplary physical layer with different channel models.**

***Index Terms*—UMICore; LTE; link level simulation; channel modelling; channel measurement.**

I. Introduction

The evaluation of mobile radio physical layer concepts under realistic channel conditions is an important contribution to the design of mobile communication systems. In this context the physical layer demonstrator *UMICore* has been developed which allows for the demonstration, visualization and training of physical layer concepts. The main focus is on adaptive coding and modulation, iterative receiver concepts as well as different channel models. The modular structure of the demonstrator allows the fast and easy integration of new components and algorithms with regard to the comparison with state-of-the-art systems. For the investigation of the UMIC physical layer aspects UMTS LTE (Universal Mobile Telecommunications System – Long Term Evolution) serves as reference.

Current releases of the UMTS LTE standard [1] feature a flexible downlink physical layer employing turbo channel coding, rate-matching, *hybrid automatic repeat-request* (HARQ), a choice of complex signal constellations (QPSK, 16QAM, and 64QAM), and cyclic prefix *orthogonal frequency division multiplexing* (OFDM).

This contribution presents the capabilities of the UMICore physical layer demonstrator using UMTS LTE exemplarily. Furthermore different channel models implemented in UMICore are described in short and evaluated regarding their influence on the UMTS LTE physical layer.

II. LTE System Model

The considered LTE transceiver (see Fig. 1) is implemented according to the physical layer specifications of the LTE standard [1]. 24 cyclic redundancy check (CRC) bits are appended to a block of $l_v = 6120$ data bits $\underline{v}$ (maximum data frame size in LTE systems [2]) which is then encoded by a systematic rate-$\frac{1}{3}$ turbo coder consisting of two parallel concatenated convolutional codes (PCCC) with octal generator polynomial $G = \{1, 15/13\}_8$ each generating one parity bit per data bit. For efficient and easy to implement rate matching, the encoded frames are interleaved and written to a ring buffer. For a given number l_v of data bits a frame of l_x encoded bits $\underline{x}$ is selected for transmission from the buffer resulting in an effective code rate $r = \frac{l_v}{l_x}$. The size l_x of the encoded bit frames is determined by a scheduler according to the user's instantaneous channel quality, the user's requested throughput, the maximum delay, the target block error rate (BLER) and the current load of the radio cell. Thereby the scheduler implicitly influences the code rate r of the user. A block size $l_x < 3 \cdot l_v$ results in a code rate $r > \frac{1}{3}$, whereas if l_x is sufficiently large, the code rate can take values $r < \frac{1}{3}$ by repetition of encoded bits.

Furthermore, the UMTS LTE hybrid automatic repeat-request (HARQ) scheme allows for up to $n_{\mathrm{HARQ}} = 4$ transmissions of different combinations of systematic and parity bits from the ring buffer, the so-called redundancy versions (RVs). For the initial transmission (RV0), first, systematic bits are selected and the remaining space of the code block of size l_v is then filled up with parity bits. Each following retransmission (RV1 – RV3) which may be requested by the receiver starts at a different position within the ring buffer, i.e., each redundancy version consists of a different combination of systematic and parity bits. Obviously, each retransmission of a code block implicitly results in a decrease of the effective code rate and directly leads to losses in throughput and latency.

The bits selected for transmission are grouped to vectors of I_m bits with $I_m \in \{2, 4, 6\}$ with $m \in \{0, \ldots, M-1\}$ representing the M subcarriers of the OFDM system. The grouped bits are then assigned to complex modulation symbols $Y_m \in \mathcal{Y}_I$ out of a signal constellation set (SCS) $\mathcal{Y}_I$, i.e. QPSK, 16QAM or 64QAM with Gray mapping. The complex modulation symbols $\underline{Y}$ are then OFDM modulated and a cyclic prefix (CP) is added to form the transmit signal $\underline{y}$ with averaged unit power. OFDM modulation is realized using an Inverse Fast Fourier Transform (IFFT) of size 2048 (corresponding to a system bandwith of $\Delta f = 20\,\mathrm{MHz}$).

Throughout this work we are considering a frequency selective multipath propagation channel causing intersymbol interference (ISI). This band limited ISI channel is modeled by a tapped delay line. The complex time variant coefficients

This work has been supported by the UMIC (Ultra High-Speed Mobile Information and Communication) research cluster at RWTH Aachen University.

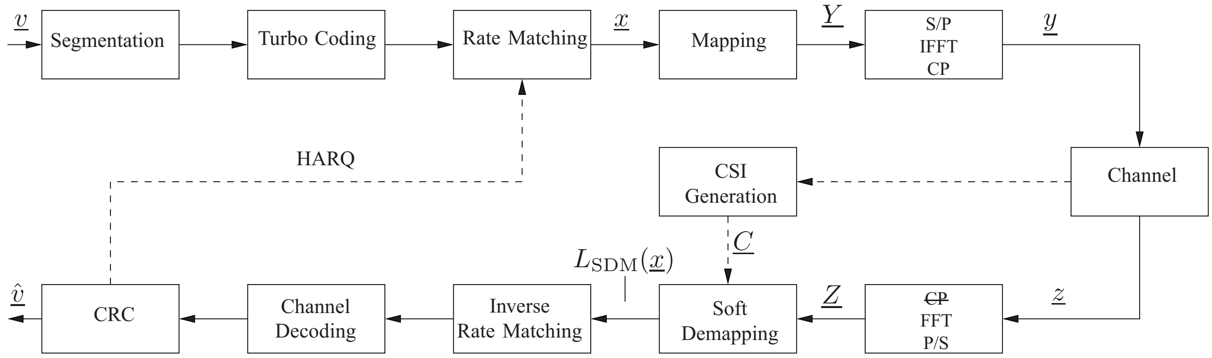

Figure 1. System model of the UMTS LTE physical layer.

$c_i(t)$ are derived from one of the channel models as described in Sec. III and fulfill

$$\mathrm{E}\left\{\|c_i(t)\|^2\right\} = 1. \tag{1}$$

The channel impulse response (CIR) $c(t, \tau)$ of length $L+1$ is given by:

$$c(t,\tau) = \sum_{i=0}^{L} c_i(t)\delta(iT - \tau),\ c_i \in \mathbb{C} \tag{2}$$

Despite the time-variant nature of the fading coefficients of each tap, we assume the channel to be constant for the duration of the transmission of one OFDM symbol. The channel is then described by a CIR vector consisting of its complex fading coefficients

$$\underline{c} = [c_0, c_1, \ldots, c_L] \tag{3}$$

which are sufficiently well estimated at the receiver. Finally, complex additive white Gaussian noise (AWGN) n with a known power spectral density of $\sigma_n^2 = N_0$ is applied.

On the receiving side the CP is removed and OFDM demodulation is performed employing the Fast Fourier Transform (FFT). The received complex symbols of each subcarrier Z_m are given as

$$Z_m = C_m \cdot Y_m + N_m,\ m \in \{0, \ldots, M-1\} \tag{4}$$

with N_m denoting Fourier transformed noise samples and C_m denoting the samples of the transfer function of length M of the channel $\underline{c}$.

$$\underline{C} = [C_0, C_1, \ldots, C_m, \ldots, C_{M-1}] \tag{5}$$

is also referred to as channel state information (CSI). It follows that after division by C_m (zero-forcing equalization) the subchannels can be regarded as individual AWGN channels with noise power

$$\sigma_{n,m}^2 = \mathrm{E}\left\{\left(\frac{N_m}{C_m}\right)^2\right\} = \frac{\sigma_n^2}{\|C_m\|^2}. \tag{6}$$

The demodulated complex symbols are fed to a soft demapper (SDM) which delivers reliability information in form of *a posteriori log-likelihood ratios* (LLR) $L_{\mathrm{SDM}}(x)$ on the encoded bits x. The LLRs are then passed on to a parallel turbo decoding structure consisting of two soft input soft output (SISO) channel decoders (CD) using the LogMAP algorithm [3] for soft channel decoding. After a fixed number of decoding iterations n_{Turbo} the data bit frame $\hat{\underline{v}}$ is hard decided from the resulting LLRs. CRC is performed and, in case of failure, a retransmission is requested.

III. Channel Models

For the evaluation of physical layer concepts under realistic or nearly realistic conditions, channel models are needed. In the UMICore demonstrator an *additive white Gaussian noise* (AWGN) channel as well as a Rayleigh fading channel are implemented as a first approximation with regard to the statistical behavior of the radio channel. The Rayleigh fading channel is based on a tapped delay line model and the rayleigh distributed fading represents the statistical properties of a channel where no line of sight exists.

Other channel models which describe the channel in a more realistic way are, e.g., the WINNER or the COST channel models. In UMICore a simplified version of the WINNER II cluster delay line (CDL) model [4] is included. This model is also based on a tapped delay line model with tabulated values, where one tap represents a cluster. One cluster consists of a number of multipaths, which have nearly the same angle of arrival and departure as well as a similar delay. Although this simplified CDL model does not yet take into account any antenna characteristics and is valid only for the SISO (single-input single-output) case it is possible to create different environmental scenarios, e.g., typical urban and rural environments under non-line-of-sight (NLOS) as well as line-of-sight (LOS) conditions.

Furthermore, for more realistic simulations, channel measurements are used. The data was obtained in an extensive channel measurement campaign at TU Ilmenau (representing a typical urban scenario). Channel sounding was performed at $2.53\,\mathrm{GHz}$ in a band of $2 \times 45\,\mathrm{MHz}$ with the RUSK TUI FAU channel sounder [5]. At the base station (BS), which served as transmitter, a uniform linear array was used with 8 dualpolarized (H/V) elements, each of them consisting of a stack of 4 patches in order to form a narrow transmit beam in elevation. At the mobile station (passenger car), a circular array with 2 rings of 12 patches with H/V polarizations was used. Additionally, a MIMO (multiple-input multiple-output) cube was placed on top. The mobile station acted as receiver. A detailed description of the measurement and antenna setups, which match the requirements of the 3GPP Long Term Evolution (LTE and LTE-A [6]) can be found in [7]. For each of the tracks and for each measured snapshot, geo-data information based on GPS, odometer and separated distance measurements via laser is available. The accuracy of the distance measurements is approximately $0.1\,\mathrm{m}$ around the start and end points of each track and $1\,\mathrm{m}$ along the measurement route. A typical length of a track is $50\,\mathrm{m}$–$70\,\mathrm{m}$. In total the measurement campaign covers 3 base station positions with a height of $25\,\mathrm{m}$ and $15\,\mathrm{m}$ and additionally a relay point ($3.5\,\mathrm{m}$) in the middle of the scenario. Only the BS height of $25\,\mathrm{m}$ is considered in UMICore. The intersite distance between the base stations is found to be $680\,\mathrm{m}$ for BS1 – BS2, $580\,\mathrm{m}$ for BS2 – BS3 and $640\,\mathrm{m}$ for BS3 – BS1. In total, more than 20 individual tracks with more than 120 measurement runs were performed. Figure 2 shows the time-variant channel state information $\underline{C}(t,m)$ in dB according to the time t and the number of subcarriers m for one exemplary track (BS1, 41a-42). One can see the strong time dependency of each subcarrier caused by the doppler effect as well as the deep fading due to the multipath propagation.

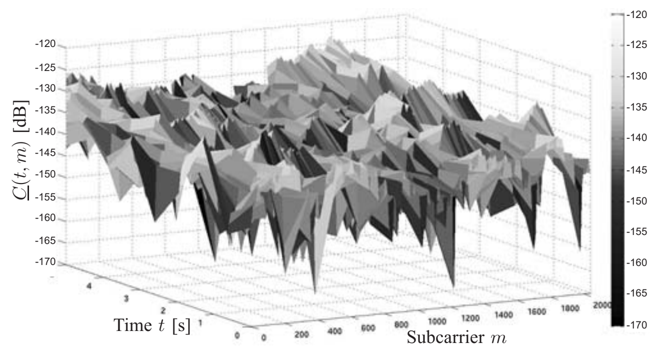

Figure 2. Channel state information $\underline{C}(t,m)$ for one exemplary track (BS1, 41a-42) of the Ilmenau channel measurements.

As UMICore only supports the SISO case so far, one antenna pair is chosen exemplarily from the measurement data. The MIMO extension of UMICore is part of the current work in progress.

IV. UMICore

The UMICore demonstrator† as depicted in Fig. 3 serves as graphical user interface of the physical layer simulation framework. Although UMICore is able to visualize different physical layer concepts (e.g. HSPA+ [8], UMTS LTE [2], WiMAX [9] or DVB-T [10]) this contribution concentrates on UMTS LTE only. UMICore allows for an interactive adaptation of all relevant physical layer parameters like (in case of LTE, cf. Tab. I) code rate, modulation scheme, number of turbo iterations or maximum number of HARQ retransmissions. The transmission is visualized by a live plot of the modulation constellation diagram (after equalization). The current bit error rate is indicated in a bar chart and illustrated by an image transmission, additionally. Further evaluation of the physical layer is enabled by plots of throughput and EXIT charts (in case of turbo codes). The user can apply different channel models (as described in Sec. III) in the physical layer simulation. The graphical user interface allows for the flexible adjustment of different channel settings listed in Tab. II as well as the depiction of the current channel state information $\underline{C}$. In case of the measured Ilmenau channel the active measurement track and the active base station can be chosen from the city map (see Fig. 4) in which the movement of the mobile station (measurement car) is depicted as well.

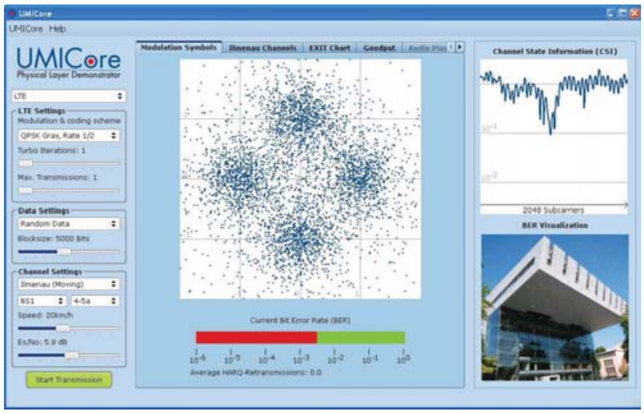

Figure 3. Screenshot of the UMICore physical layer demonstrator.

Table I
SETTINGS FOR THE UMTS LTE PHYSICAL LAYER IN UMICORE.

Code rate	$r \in \{1, \frac{1}{2}, \frac{1}{3}, \frac{2}{3}, \frac{3}{4}, \frac{5}{6}, \frac{7}{8}\}$
Modulation scheme	QPSK, 16QAM, 64 QAM (Gray mapping)
Turbo iterations	$n_{\mathrm{Turbo}} \in (1 \ldots 10)$
HARQ retransmissions	$n_{\mathrm{HARQ}} \in (1 \ldots 4)$

Table II
CHANNEL SETTINGS FOR DIFFERENT CHANNEL MODELS IN UMICORE.

AWGN	signal-to-noise-ratio (E_S/N_0)
Rayleigh Fading	none
Simplified WINNER II	propagation environment (rural, urban, in-door), each with LOS/NLOS
Ilmenau Channel	measurement track, base station

V. Simulation Results

In the following the performance of the UMTS LTE system with a fixed code rate $r = \frac{1}{3}$ shall be evaluated exemplarily for different channel settings. Figure 5 compares the bit error rates (BER) of the UMTS LTE system for an AWGN channel and for the measured Ilmenau channel. Obviously the AWGN channel yields a better performance than the Ilmenau channel since the latter enables a more realistic reconstruction of

†A light version of the UMICore demonstrator is available for download on http://www.ind.rwth-aachen.de/umicore

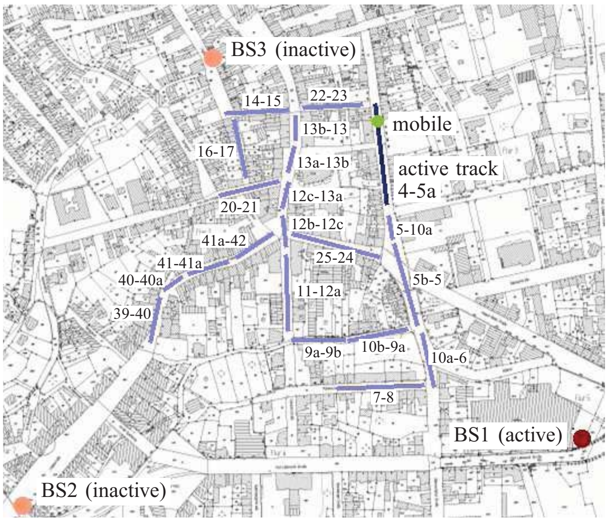

Figure 4. City map of Ilmenau: user interface for the measured Ilmenau channel in UMICore.

the radio channel incorporating doppler effect and multipath propagation.

Figure 6 shows the throughput of the different schemes in terms of bits per channel use $\mathcal{B}$ which is defined as

$$\mathcal{B} = \frac{(1 - \mathrm{FER}) \cdot rI}{n_{\mathrm{HARQ}}} \tag{7}$$

with the frame error rate FER. For both channel models the four throughput levels caused by the HARQ retransmissions are clearly visible. The throughput curves confirm the bit error rate simulations in Fig. 5 since the better performance of UMTS LTE under AWGN channel conditions is still evident. The gap between the two throughput curves widens for higher order modulation schemes because they are more susceptible to distortions caused by fading effects inherent to the measured Ilmenau channel.

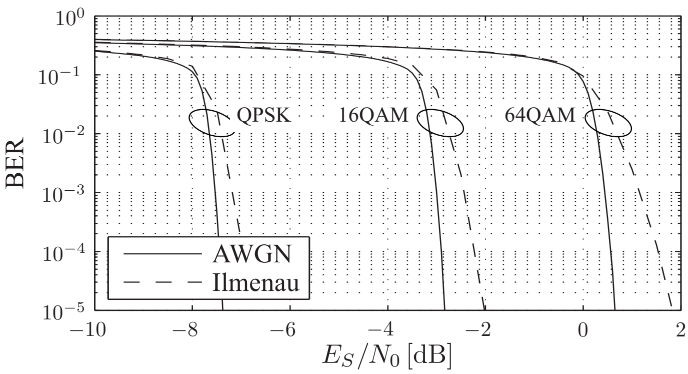

Figure 5. Bit error rates for different channel models ($r = \frac{1}{3}$, 10 turbo iterations, max. 3 HARQ retransmissions).

VI. Conclusion

In this paper the UMICore physical layer demonstrator was presented, a software tool which is very well suited for the demonstration and visualization of various physical layer concepts as well as channel models. The software tool

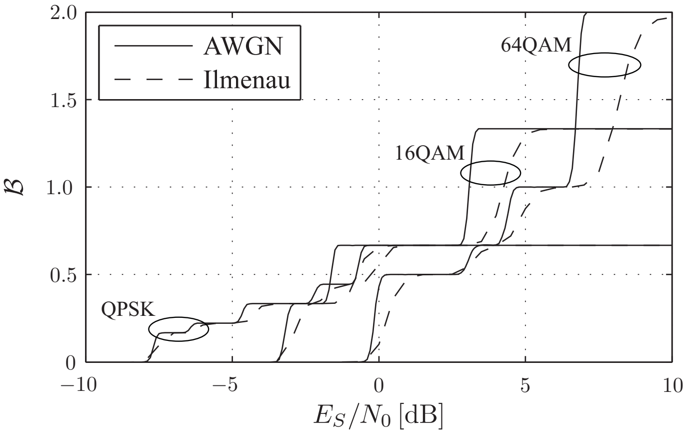

Figure 6. Bits per channel use $\mathcal{B}$ for different channel models ($r = \frac{1}{3}$, 10 turbo iterations, max. 3 HARQ retransmissions).

provides a fast overview of the influence of different physical layer parameters or channel settings. Characteristics, e.g. the bit error rate or throughput, of various system settings can be analyzed and illustrated in a clear and intuitive way. The capabilities of UMICore have been presented exemplarily by a comparative analysis of UMTS LTE for different radio transmission channels.

VII. Acknowledgments

The authors would like to thank Laurent Schmalen for providing parts of the software basis used in the simulation tool.

References

[1] 3rd Generation Partnership Project (3GPP); Technical Specification Group Radio Access Network, "Evolved Terrestrial Radio Access (E-UTRA) and Evolved Universal Terrestrial Radio Access Network (E-UTRAN); Overall description; Stage 2," TS 36.300, Version 8.9.0, July 2009.

[2] 3rd Generation Partnership Project (3GPP); Technical Specification Group Radio Access Network, "Evolved Terrestrial Radio Access (E-UTRA); Multiplexing and Channel Coding," TS 36.212, Version 8.2.0, Rel. 8, Mar. 2008.

[3] L. Bahl, J. Cocke, F. Jelinek, and J. Raviv, "Optimal decoding of linear codes for minimizing symbol error rate (corresp.)," *IEEE Transactions on Information Theory*, vol. 20, no. 2, pp. 284–287, Mar. 1974.

[4] P. Kysti et al, "WINNER II Channel Models," IST-4-027756 WINNER II D1.1.2 V1.2, Feb. 2008, http://www.ist-winner.org.

[5] "The RUSK TUI FAU Channel Sounder," 2010, http://www.medav.de.

[6] 3rd Generation Partnership Project (3GPP); Technical Specification Group Radio Access Network, "Requirements for Further Advancements for E-UTRA (LTE-Advanced)," TS 36.913, Version 8.0.0, Rel. 8, June 2008.

[7] C. Schneider et al, "Multi-User MIMO Channel Reference Data for Channel Modelling and System Evaluation from Measurements," in *IEEE Workshop on Smart Antennas (WSA)*, Berlin, Germany, 2009.

[8] 3rd Generation Partnership Project (3GPP); Technical Specification Group Radio Access Network, "Technical Specification Group Radio Access Network; Physical layer – General description," TS 25.201, Version 9.0.0, Rel. 9, Dec. 2009.

[9] IEEE Computer Society, "IEEE Standard for Local and metropolitan area networks; Part 16: Air Interface for Broadband Wireless Access Systems," IEEE Std. 802.16-2009, June 2009.

[10] European Telecommunications Standards Institute (ETSI), "Digital Video Broadcasting (DVB); Framing structure, channel coding and modulation for digital terrestrial television," EN 300 744, Version 1.6.1, Jan. 2009.